



# Differential Expression of Growth and Differentiation Genes in Murine Parotid Gland-Derived Stem Cells Cultured on Three-Dimensional Alginate Hydrogel

## ARTICLE INFO

### Article Type

Original Research

### Authors

Malaki M.<sup>1</sup>

Tiraihi T.<sup>1\*</sup>

Ghorbani-Anarkooli M.<sup>1</sup>

Babaei A.<sup>1</sup>

Department of Anatomical Sciences,  
Faculty of Medical Sciences, Tarbiat  
Modares University, Tehran, Iran.

### \*Corresponding author:

Tiraihi T

Department of Anatomical Sciences,  
Faculty of Medical Sciences, Tarbiat  
Modares University, Tehran, Iran.

Email: takialtr@modares.ac.ir

## ABSTRACT

**Introduction:** We aimed to compare the gene expression of parotid gland derived stem cell in a three (3D) alginate hydrogel culture with that of a two-dimensional one (2D).

**Materials and methods:** Five rats were sacrificed and the parotid glands were removed and cultured in DMEM/F12 medium supplemented with 15% FBS. The cells were characterized by flow cytometry and immunocytochemistry for evaluating the expression of genes. The cells were encapsulated in alginate hydrogel, then the differentiation was compared with that of a 2D culture. qRT-PCR was performed in order to evaluate the expression of Amy1, Cldn3, Cldn4, Ki67, Cyclin D1, Dpt, Meox2, Aquaporin 5, Pparg, Bpifa2e and Tp63 genes.

**Results:** The harvested cells immunoreacted with CD90, CD44, and CD29, however, the immunophenotyping of CD45 and CD34 were negative. The immunocytochemistry results showed that they were strongly immunostained with K-7 and E-cadherin, but less with K-14. In the 3D culture, the cells differentiated into organoid bodies with round shape, there was duct-like structure extended from one pole. The qRT-PCR in the 3D culture showed increase in the expression of Amy1, Ki67, aquaporin5, Pparg, Bpifa2e and Tp63 genes compared to 2D culture. In contrast Cldn3, Cldn4, cyclin D1, Dpt and Meox2 genes were strongly expressed in the 2D culture.

**Conclusion:** The results of flow cytometry and immunocytochemistry confirmed the properties of the isolated cells were parotid gland-derived mesenchymal stem cells. They differentiated into organoid body in the 3D culture using alginate as scaffold which expressed parotid gland differentiation genes.

**Keywords:** Parotid gland, Alginate, Stem cell, Organoid.

Copyright© 2020, TMU Press. This open-access article is published under the terms of the Creative Commons Attribution-NonCommercial 4.0 International License which permits Share (copy and redistribute the material in any medium or format) and Adapt (remix, transform, and build upon the material) under the Attribution-NonCommercial terms

## INTRODUCTION

Dry mouth can be caused by several conditions such as Sjögren syndrome and radiation therapy [1-3], one of the approaches is transplantation of salivary gland cells in the injured gland [4], while other investigators transplanted salivary gland cells differentiated from mice embryonic stem cells [5]. Recently, salivary gland organoid bodies have been used as transplants in order to restore the physiological function of the salivary gland [6]. These organoid bodies were also

expected to be a promising tool for disease modeling, drug discovery and regenerative medicine in salivary glands [7]. Moreover, several investigators considered salivary gland morphogenesis as an *in vitro* model for salivary gland biology by forming organoid structures [8-12]. This model has been used in transplantation experiments [13], however, due to the limited growth and self-renewal capacity of the salivary gland stem cell [14], an alternative approach using organ bioengineering has been considered

[15-18]. The most challenging part of acinar cell culture was the paucity of the cells [18, 19], therefore, the use of a suspended cell culture could aggregate to form a 3D sphere in tissue culture, this culturing system could improve cell survival, proliferation, and function [20]. Tissue engineering is an approach to generating artificial glands using acinar epithelial cells with a supporting scaffold, this can be applied for constructing glandular structure using a 3D culture. Natural or synthetic hydrogels were utilized as scaffolds because they resembled extracellular matrix. For example, several synthetic polymers were used such as polycaprolactone and poly ethylene glycol as scaffolds in salivary gland tissue engineering [21].

On the other hand, there are many genes involved in parotid gland development in rodents, for example, early growth response 1, mesenchyme homeobox 2 and dermatopontin (Dpt), Egr1 and Meox2 genes. They are expressed during embryogenesis and are responsible for the fate determination of the parotid gland in mouse embryo [22], whereas Aquaporin 5 gene is considered a differentiation marker for proacinar cells [23]. Pparg gene, a transcription factor, transiently increases during mid-postnatal of parotid acinar cell differentiation, however, adult parotid acinar cells do not express Pparg gene [2, 23]. Alpha-amylase and parotid secretory proteins (Bpifa2e gene) are known as terminal differentiation markers [2]. These genes are considered in this investigation for evaluating parotid gland cell differentiation and growth in the 3D culture. Some genes are considered for evaluating cell growth and proliferation, such as Ki67, a protein with a half-life of only ~1-1.5 h and is present during all active phases of the cell cycle (G1, S, G2 and M), but it is absent in resting cells (G0 phase) [24]; Cyclin D1, a key cell-cycle regulatory protein required for the cell progress through G1 to S phase, is also considered in this study [25].

We intend to investigate the growth and differentiation genes of parotid cell cultured in an alginate 3D scaffold. The expression level of Amy1, Cldn3, Cldn4, Ki67, Cyclin D1, Dpt, Meox2, Aquaporin 5, Pparg, Bpifa2e and Tp63

genes will also be evaluated. Moreover, the differential gene expression between the two-dimensional culture (2D) of parotid gland-derived cells and those encapsulated in alginate hydrogel will be investigated.

## MATERIALS AND METHODS

### Animals

Five rats (6 to 8 weeks) were housed in the Tarbiat Modares University animal facility under controlled humidity, temperature, and a 12 hours light/dark cycle. They were fed on standard diet with freely available food and sterile water. All of the animal experiments were approved by the Faculty of Medical Sciences ethical committee at Tarbiat Modares University (IR.MODARES.AEC.1401.030). From each sacrificed rat, tissue was sampled and confirmed that they it was were a parotid gland.

### Preparation and characterization of parotid gland-derived cells

The parotid gland-derived cells were isolated and cultured by mincing the gland into small pieces followed by enzymatic digestion (1 mg/mL collagenase type I: Invitrogen, Eggenstein, Germany) for 30 minutes and then the digestion medium was discarded. The isolated cells were washed with 5 mL of DMEM/F12 (Invitrogen, Eggenstein, Germany) three times and were seeded into a dish in the same medium supplemented with 15% FBS (GIBCO; Paisley, UK), incubated in a 5% CO<sub>2</sub> incubator at 37 °C and cultured for three days. On Day 3, the medium was replaced with a fresh one. On Day 7, the adherent cells were harvested by digestion with Trypsin/EDTA (0.05% trypsin and 0.02% EDTA: Invitrogen, Eggenstein, Germany). The cells at passage 3 were used for 2D and 3D cultures.

Characterization of the cells was done by harvesting the cells in trypsin/EDTA, then they were washed twice with phosphate buffer solution, resuspended and evaluated by flow cytometry for the following markers: CD90 (anti-CD90 mouse monoclonal antibody, abcam, Cambridge, UK); CD44 (anti-CD44 mouse monoclonal antibody, abcam, Cambridge, UK); CD29 (anti-CD29 mouse monoclonal antibody,

abcam, Cambridge, UK); CD34 (anti-CD34 mouse monoclonal antibody, abcam, Cambridge, UK) and CD45 (anti-CD45 mouse monoclonal antibody, abcam, Cambridge, UK) [26]. Another set of cells were subjected for immunocytochemistry using antibodies against keatin-7, E-cadherin and keratin-14.

### Immunocytochemistry

The cells in the 2D culture were seeded on a cover slip for one week, washed in phosphate buffer solution (pH 7.2), fixed in buffered paraformaldehyde (4%), washed twice in phosphate buffer solution, treated with 10% goat serum (to prevent nonspecific reactions), inhibited for endogenous peroxidase ( $\text{H}_2\text{O}_2$ : 3%), permeated with triton x100 (0.3%: Sigma-Aldrich, St. Louis, MO), labeled with primary antibodies, incubated with peroxidase conjugated secondary antibody and examined under a photomicroscope, respectively.

The primary antibodies are as follows: Mouse anti- E-cadherin monoclonal antibody (1/500; abcam, Cambridge, UK), Rabbit anti-K7, polyclonal antibody (1/500; abcam Cambridge, UK), Rabbit Anti-K14, polyclonal antibody (1:500; abcam Cambridge, UK) Rabbit anti-mouse, polyclonal antibody conjugated with peroxidase (1:500; abcam Cambridge, UK) and goat anti-rabbit, polyclonal antibody conjugated with peroxidase (1:500; abcam Cambridge, UK) [27].

### Preparation and characterization of alginate hydrogel

In order to encapsulate the cells with alginate hydrogel, alginate (0.1 g) was dissolved in DMEM/F12 medium (1.0%: w/v), the cross-linker ( $\text{CaCl}_2$ ) was added (volume ratio for 1% alginate:  $\text{CaCl}_2$ ; 10:1), the alginate hydrogel was formed by stirring for 5 hours [28].

### Characterization of alginate hydrogel Scanning electron microscopy

The samples from alginate hydrogel and encapsulated cell alginate hydrogel were lyophilized by a freeze dryer (Martin Christ, Osterode am Harz, Germany) for 24 h. The dry encapsulated cell/hydrogel was coated with gold and analyzed by SEM at 15 kV (Zeiss 912 Omega (Oberkochen, Germany) [29].

### Swelling ratio of the hydrogel

The alginate powder was dissolved in deionized water by stirring at room temperature (RT) for 12 h. The resulting aqueous was 1.0% solution of alginate hydrogel, which was formed by pouring the alginate solution on a glass coverslip and placing it in a 15 mL cross-linking solution; then the cross-linking solution was removed before weighing the hydrogel, which was measured by subtracting the weight of the coverslip. The cumulative mass of a glass-gel sandwich was measured and the average weight of the glass coverslips was subtracted so as to obtain the hydrogel's mass. At least three independent samples were prepared for every experiment [30].

### Encapsulation of cells in alginate hydrogel

The cells were ( $5 \times 10^5/\text{mL}$ ) mixed with the prepared alginate solution (using DMEM/F12 supplemented with 15%), then dripped in the cross-linker  $\text{CaCl}_2$  solution, where the final  $\text{CaCl}_2$  solution was a 1%. The alginate hydrogel disks were washed in phosphate buffer solution and transferred to a 37 °C incubator with 5%  $\text{CO}_2$  and 95% moisture [31].

### MTT assay

This experiment tries to evaluate the cytotoxicity and survival of encapsulated cells in the alginate hydrogel and the control groups. The cultured cells were placed on the bottom of a 96-well plate and were cultured for 1, 3 and 7 day(s) so as to evaluate the viability (comparing between 2D and 3D groups). The supernatant was removed, and then 150  $\mu\text{L}$  of MTT solution was added to each well and incubated for 4 hours at 37 °C. After 4 hours, the MTT solution was removed from the wells and 100  $\mu\text{L}$  of DMSO (dimethyl sulfoxide) was added on each well. After converting the purple crystals to a soluble form in DMSO. absorption by Elisa reader at 570 nm was evaluated [32].

### qRT-PCR

The gene expression was evaluated by quantitative reverse transcriptase polymerase chain reaction (qRT-PCR) performed on the encapsulated cells seeded in the 2D culture (21 days). The control was the cells seeded in the 2D culture at day zero. The following genes were

used in the study: Amy1, Cldn3, Cidn4, Ki67, Cyclin D1, Dpt, Meox2, Aquaporin 5, Pparg, Bpifa2e and Tp63 genes. GAPDH was used as a housekeeping gene (internal control). The primers were designed using primer3 software version v. 0.4.0 (<https://bioinfo.ut.ee/primer3-0.4.0/>).

The sequences of the primers and fragment size are listed in table 1. The cells were lysed using the ready Cell Lysis Kit (Roche, Basel, Switzerland), then RNA extraction was performed (Trizol reagent; Invitrogen, Germany), and the solution was added to the microtube containing the cells. After 5 minutes of incubation on ice, 200  $\mu$ l of chloroform was added to the solution and shaken for 15 seconds, then centrifuged at 4 °C for 15 minutes at 12000 RPM, forming three phases, the upper phase being clear and containing the RNA, it was removed, mixed with an equal volume of isopropanol and incubated for 15 minutes at 4 °C and then centrifuged at the same temperature for 15 minutes at 12000 rpm. Seventy percent ethanol was added to precipitate the RNA, and after vortexing, it was centrifuged at 7500 rpm for 4 minutes at 4 °C. After drying the alcohol (20 microliters of the DEPC-treated water (0.1%)) were added to the precipitate, and after a short centrifugation, it was incubated for 60 minutes at 60 °C and then stored in a freezer at -80 °C. In order to avoid possible contamination of the RNA with the DNA, the solution was treated with RNase-free DNase enzyme and the purity and concentration of the RNA were checked. cDNA synthesis was performed according to the protocol of the manufacturer (Fermentas, USA) and finally the RT-PCR reaction was performed by mixing 10  $\mu$ l of Master Mix 2X and 25 ng of cDNA with forward and reverse primers with a thermal cycler T100

(Bio-Rad Laboratories, Hercules, CA). The evaluations were performed three replications and were expressed as mean  $\pm$  standard deviation (SD) [33].

### Statistical analysis

The results of this study are statistically analyzed by SPSS (V16, 2016; IBM, USA). The results of the genes quantitative study were evaluated by One Way ANOVA statistical test, the difference between the means was considered significant at the level of  $P \leq 0.05$ .

## RESULTS

### Cell isolation and characterization

The parotid glands were exposed and removed from five rats at 6-8 weeks of age, they were sacrificed according to the guidelines of the ethical committee of Faculty of Medical Sciences at Tarbiat Modares University. A small piece from each parotid gland was sampled and confirmed by a histological technique (Fig. 1). The collected parotid glands were cut in small pieces and the cells were isolated by enzymatic digestion (collagenase type 1). Then, they were cultured in DMEM/F12 supplemented with 15% FBS. The primary culture showed many free-floating cells (Fig. 1-B). Figure 1-C shows cells cultured for three days, adherent with heterogenous morphology. They were characterized by flow cytometry. CD44, CD90 and CD29 markers were highly expressed, while the expression of CD45 and CD34 was negative. (Fig. 2 A-E). Figure 2-F shows the histogram of immunophenotyping, the mean and standard deviation of CD90, CD44 and CD29 The immunopositive cells were  $99.10 \pm 3.1\%$ ,  $98.57 \pm 3.9\%$  and  $98.57 \pm 2.4\%$ , respectively.

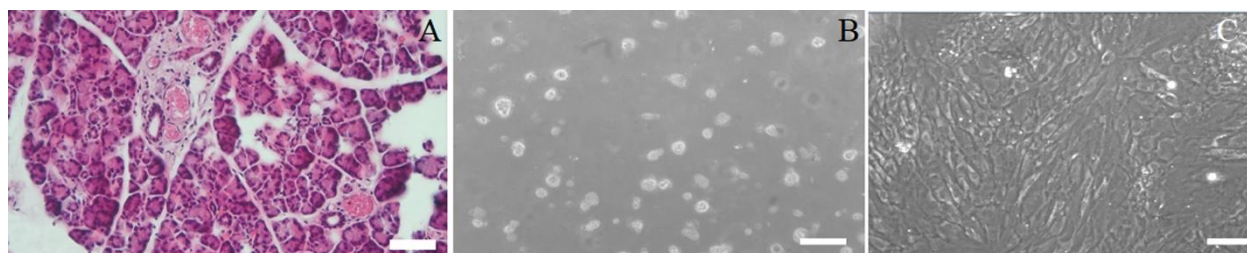


**Fig. 1.** Morphology of the murine parotid gland and the cultured cells A: a parotid gland fixed in formalin, embedded in paraffin and stained with Hematoxylin and Eosin. B: The primary culture of the isolated parotid cells. They are round in shape. C: The morphology of parotid gland cells cultured for 3 days. They are heterogenous in shape, many are spindle and others are round or stout in shape. (Scale bar: A=90, B=1000 and C= 90  $\mu$ m).



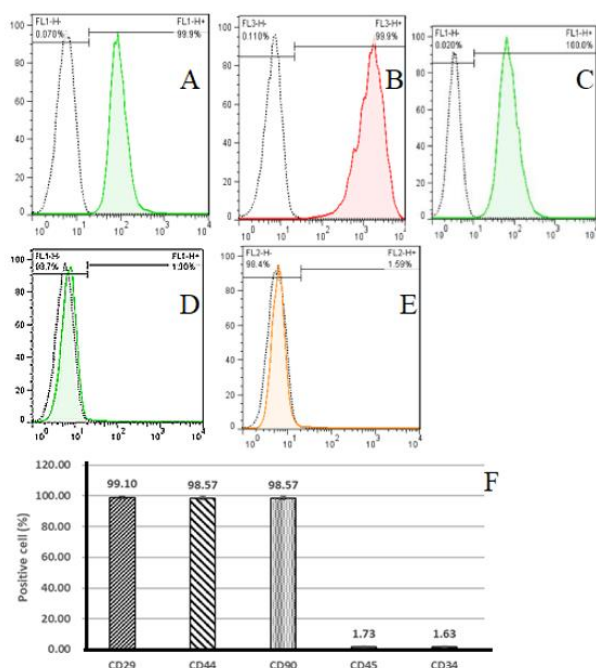


**Fig. 2.** Characterization of the isolated cells by immunophenotyping using flow cytometry of mesenchymal stem cell-specific antibodies comprising CD44 (A) and CD90 (B), salivary gland specific antibody of CD29 (C)

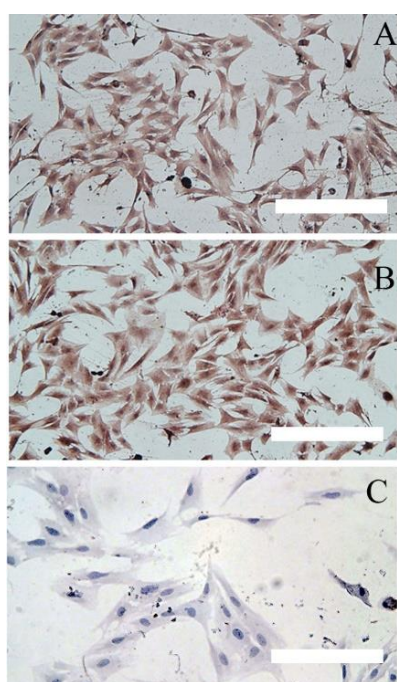


**Fig. 3.** Epithelial cell marker expression in the cells. A: Immunostaining with keratin-7. B: Immunostaining with E-cadherin. C: Immunostaining with keratin-14. Scale bar = 100 μm).

The cells in the 2D culture were stained for the epithelial cell markers, keratin-7 and E-

cadherin, which showed a high level of immunoreactivity, while keratin-14 showed a low level of immunostaining (Fig. 3).

### Characterization of alginate hydrogel

The prepared alginate hydrogel was examined under scanning electron microscope (Fig. 4-A). The hydrogel was porous with a mean pore size of 220μm. Figure 5-A demonstrates the swelling rate of the hydrogel which shows a logarithmic trend of increase in the swelling ratio up to 40th minute then it changed to a very slow rate. The MTT assay shows that there were no statistical differences in the viability of the cells seeded at day(s) 1, 3 and 7 in the 2D culture, while in the 3D culture, the cells showed the highest viability at day 1, then slightly declined at day 3, and afterwards slightly increased at day 7. Figure 5 demonstrates the viability of the encapsulated cells, which were higher in the 2D culture than the 3D one.

### Encapsulation of the cells

The encapsulated cells in alginate hydrogel are presented in Fig. 6 at both low magnification (Fig. 6-A) and higher magnification (Fig. 6-B). The encapsulated cells are located under the hydrogel surface, they are round in shape with sharp borders (arrows). The cells in the hydrogel were stained with vital stain (acridine orange), and most of the cells were stained with green fluorescent color, which indicates that most of the cells survived after culturing for 10 days (Fig. 7-A). They were also counterstained with propidium iodide (Fig. 7-B), and few cells were stained with red fluorescent color in the hydrogel cultured for 10 days, which indicates that they were dead cells. These two images were merged in order to show the amount of survived and dead cells, there were few dead cells with yellow fluorescent color.

### Organoid bodies formation

Figure 8 shows the cells differentiated into organoid bodies of the salivary gland (Fig.8-o), where the round salivary acinus-like structure had a polar structure extended from the pole of these acini forming a duct like structure (Fig 8-d). Some cells were aggregated in order to form an early stage of acinus formation (Fig. 8-e).

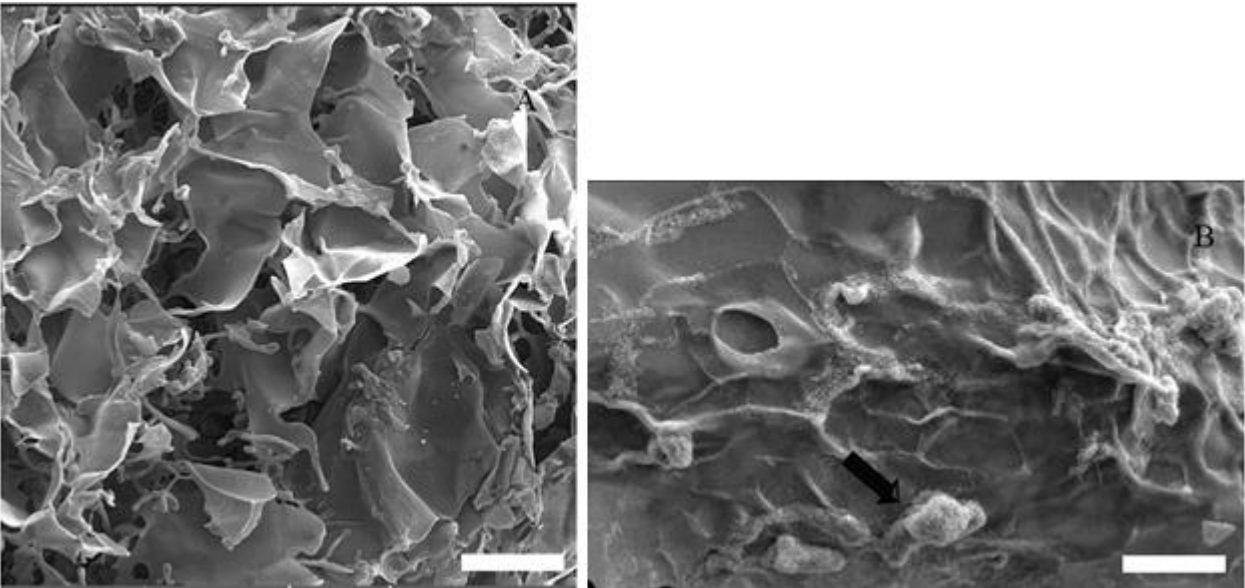


**Fig. 4.** Scanning electron microscopy of the hydrogel. A: the image shows the porous scaffold. B: represents the encapsulated cells in alginate hydrogel (Scale bar = 500 μm).

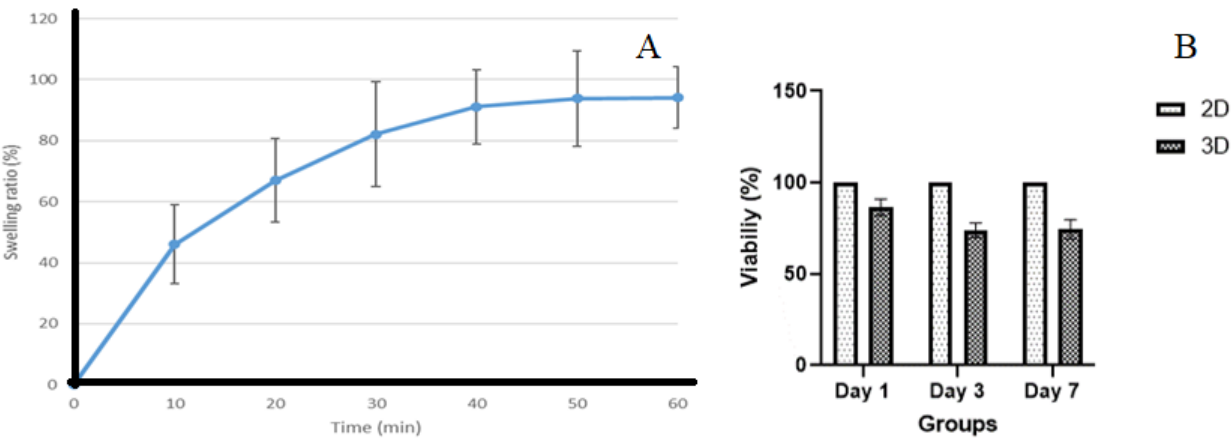


**Fig. 5.** The swelling ratio of the alginate hydrogel (A), while the cytotoxicity of the encapsulated cells in alginate hydrogel (B).

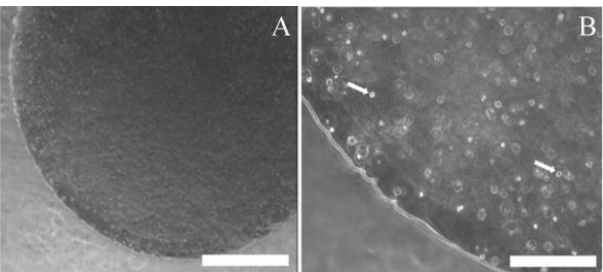


**Fig. 6.** The encapsulated cells in alginate hydrogel, arrow indicates an encapsulated cell in the hydrogel. (Scale bar A= 500, B= 250 μm).

### Gene Expression Profile

The expression of the genes in the cells in the 2D and 3D cultures was done using qRT-PCR. Obtained results indicated that the gene expression in cell growth gene Ki67 and cell cycle regulation gene cyclin D1 was not similar. Cyclin D1 was highly expressed in the 2D culture, in contrast to Ki67 which was highly expressed in the 3D culture.



**Fig. 7.** The encapsulated cells are stained with acridine orange (A), propidium iodide (B), then they merged to show the survival of the encapsulated cells in alginate hydrogel (C). (Scale bar = 125  $\mu$ m).

On the other hand, Amy1 gene was highly expressed in the 3D culture (50 times higher in 3D culture compared to the 2D one), similar pattern of expression was noticed in BPIFA2 gene, which is also known as parotid secretory protein, Cldn3 and Cldn4 genes, tight junction proteins, dermatopontin (DPT) gene, is extracellular matrix protein, and Meox2 protein, which is involved in fate determination of the salivary gland during embryogenesis. Other genes were evaluated in this study, Pparg gene, which is involved in regulating parotid acinar cell terminal differentiation; and Tp63 gene which maintains regulatory mechanisms in epithelial cells differentiation. Both genes were highly expressed in the 3D culture (see Fig. 9).

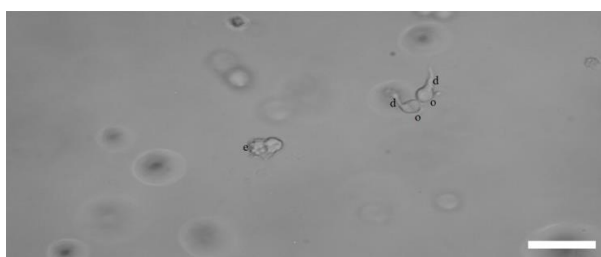


**Fig. 8.** The encapsulated cells formed organoid with an acinus-like structure (o) and duct (d), while e represents an early stage of the organoid structure. (Scale bar = 160  $\mu$ m).

## DISCUSSION

In this study, alginate hydrogel is used as scaffold in the 3D culture system. Parotid gland derived mesenchymal stem cells were encapsulated in alginate hydrogel. After 4 days, the cells integrated in the scaffold, and after 10 days, acinus-like organoid bodies were noticed, while the gene profiling showed an increase in the expression of growth and differentiation

genes. Characterization of the alginate hydrogel is consistent with our previous results [28].

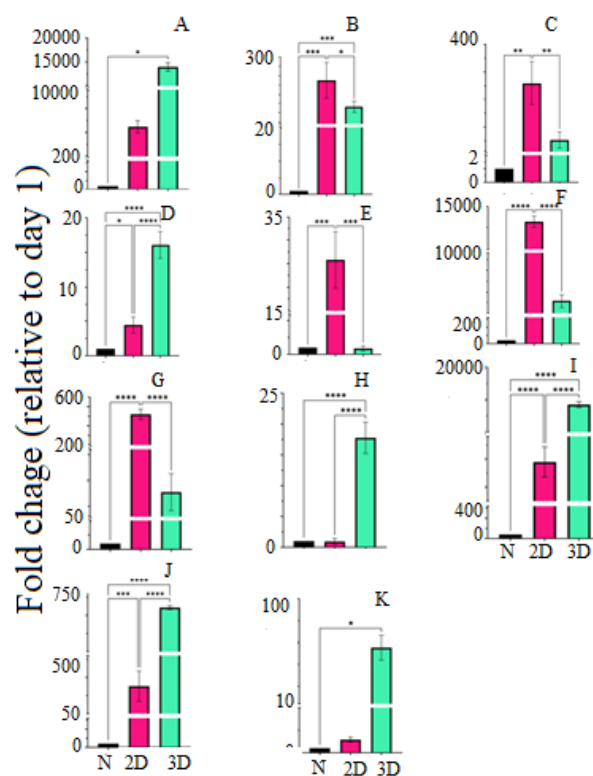


**Fig. 9.** shows the expression of the genes in the controls (N), isolated parotid gland cells at day zero incubation time, the isolated parotid gland cells at the end of 10-day incubation time (two-dimensional culture group: 2D) and the encapsulated cells in alginate hydrogel (three-dimensional culture group: 3D). A, B, C, D, E, F, G, H, I, J and K represent Amy1, Cldn3, Cldn4, Ki67, Cyclin D1, Dpt, Meox2, Aquaporin 5, Pparg, Bpifa2e and Tp63, respectively. The expression of the genes in the 2D and 3D cultured cells. The later shows an increase in the expression of Amy1, Ki67, aquaporin5, Pparg, Bpifa2e and Tp63; whereas Cldn3, Cldn4, cyclin D1, Dpt and Meox2 were expressed at a high level in the 2D culture group compared with 3D one. \*: significance level is 0.001; \*\*: significance is level 0.005; \*\*\*: significance level is 0.01 and \*\*\*\*: significance level is 0.05 (All comparisons are statistically significant).

However, the viability of the encapsulated cells was lower than that of 2D culture at the first and third days. A similar finding was noticed by Siburian [34]. This may be due to the change in the metabolism resulted from treating the cells which was reported as the MTT method's limitation [35-38].

The advantage of using alginate hydrogel as a scaffold for the 3D culture of the salivary gland is that it provides stability for growth of the salivary gland epithelium [39]. Hajiabbas et al. concluded that arginine-glycine-aspartic acid-modified alginate-based hydrogels, egg white-alginate blend and chitin/chitosan-based scaffolds provided a suitable environment for enhancing submandibular salivary gland growth and differentiation [40].

The Parotid gland derived organoid bodies were reported by other investigators [41]. In this investigation, the culture medium was supplemented with 15% FBS. Most research supplemented the culture medium with growth factors and inducers. For example, FGF-2 combined with laminin-enriched basement membrane extract or laminin-111 was used for culturing mouse submandibular gland organoids [42]. Other investigators used FGF combined with retinoic acid in order to generate submandibular gland organoids (Kim et al., 2021), while Tanaka et al. utilized bone morphogenetic protein 4 (BMP4) and SB431542 (an inhibitor of transforming growth factor- $\beta$ ) in order to induce human induced pluripotent stem cell into salivary gland organoids [3]. Parotid gland organoid was generated by epidermal growth factor, fibroblast growth factor-2, N2, insulin, and dexamethasone, and the cells seeded on polymerized Matrigel [41]. Zhao revealed that salivary gland organoids derived from embryonic stem cells were achieved by applying a two-step protocol [43]. An initial induction of embryonic stem cells into oral ectoderm by exposing the cell to BMP4, TGF $\beta$ -i, BMP1, and FGF2 followed by induction with FGF7 and FGF10; moreover, salivary gland organoids can also be generated from adult stem cells cultured on extracellular matrix combined with cytokines and FGF, Wnt3a, R-spondin 1, and TGF $\beta$ -i. (Zhao et al., 2021).

In this study, we intended to induce parotid gland organoid bodies by selecting a population of stem cells that can grow without growth factor(s) dependency. By avoiding growth factor exposure, we allowed the cells to grow and differentiate under a natural condition supported by alginate scaffold and supplemented with 15% FBS. Culturing cells in a medium supplemented with growth factor(s) resulted in growth factor(s) dependency [42, 44, 45]. Growth factor dependent cells may undergo apoptosis following growth factor withdrawal [46, 47].

Cells derived from mouse parotid gland failed to survive, unlike those of rats, which may be due to the species difference (CHEN et al. 1983; Karn et al. 2013). We suggest that the cultured mouse salivary gland cells require growth factor(s) for their survival.

In this study, immunophenotyping of the cells positively reacted to CD44 and CD90, which are mesenchymal stem cell markers, moreover, they were also immunopositive to CD29 (salivary gland specific antibody). Moreover, the cells were immunostained with K7, E-cadherin and K14. Figure 3 demonstrates the epithelial cell markers expression in the cells. The results show that immunostaining with keratin-7 and E-cadherin was highly expressed which may indicate the epithelial property of the isolated cells. We conclude that we obtained parotid gland mesenchymal stem cells [48]. While Rotter et al. identified adult stem cells with mesenchymal characteristics in human parotid gland tissues [49], Yi et al. isolated and purified multipotent epitheliomesenchymal stem cells, immunoreactive mesenchymal and epithelial markers, from human parotid gland. The results of our investigation is consistent with their finding [50].

### Gene Expression

Savatier and Malashicheva documented that cyclin D1 gene is a mitosis regulator, and that its expression was very low in 3D culture [51]. The results are consistent with those of Skrobanska et al., who reported strong suppression of cyclin D1 expression in the 3D culture. On the other hand, Ki67 gene was highly expressed in the 3D culture [52], which indicates that many cells lost



their contact inhibition mechanism as a result of cell migration in the scaffold [53].

Amy1 gene expression was very high in the 3D culture, it is considered as a marker of functionality [54]. In addition to that, BPIFA2 gene, a parotid secretory protein, was expressed in the parotid gland similar to Amy1 expression pattern. We noticed that it was expressed in the 3D culture higher than the 2D one, this pattern of expression of both genes (Amy1 and BPIFA2) confirmed that the encapsulated cells differentiated in the organoid bodies. Metzler et al. reported that gaining dense granules resulted from the expression of salivary proteins such as amylase and parotid secretory protein (BPIFA2 gene) associated with an increase in polarity of parotid epithelial cells resulting in acinar cell full maturity [2]. Also, after the differentiation of parotid gland with the establishment of the cellular polarity, AQP5 gene was expressed exclusively at the apical membrane of serous acini, which was detected during both pre- and post-natal development [55]. The Pparg gene was highly expressed in the 3D culture, which transiently increased during the mid postnatal differentiation [2]. TP63 gene is a transcription factor involved in development and homeostasis of epithelia, moreover, it was reported to maintain salivary gland stem/progenitor cell function [56], the level of Tp63 was significantly high in the 3D culture compared with the 2D one. Kouwenhoven et al. reported that regulatory mechanisms in epithelial cells were arranged and performed by Tp63 gene [57].

Meox2 gene, involved in fate determination of the salivary gland during embryogenesis, showed significantly higher level of expression in the 2D culture, expressed at early stages of parotid gland development, indicating that alginate hydrogel enhances the morphogenesis of the parotid gland [22]; moreover, DTP gene had similar pattern of expression, it was associated with fibronectin in inducing duct-like elongation during initial stages of salivary gland bud formation [58].

Both Cldn3 and Cldn4 are tight junction proteins and they have a similar pattern of expression in the 2D culture. They were highly expressed in most of the normal epithelial cells, other organs such as the brain had distinctive

Cldn expression profiles, where Cldn3 and 4 were expressed at low levels but Cldn2 was highly expressed (Hewitt et al., 2006). We expected the expression of Cldn3 and 4 in the 3D culture to be high, however, their low level of expression could be caused by the absence of growth factor(s), and variation in culture conditioning. For example, in the primary culture of parotid, the expression pattern of these proteins remarkably changed, where a high level of cldn4 expression was noticed, while the level of Cldn3 was low. Moreover, in rodents, the acinar cells of salivary glands expressed cldn3 but not Cldn4, whereas duct cells expressed both. The distinct Cldn expression patterns may reflect differences in the permeability of tight junctions.

## CONCLUSION

We concluded that 3D culture of parotid gland-derived stem cell using alginate as scaffold induces the expression of growth and differentiation genes with formation of organoid bodies.

## CONFLICTS OF INTEREST

All the authors declare that there no conflict of interest.

## AUTHORS DISCLOSURE STATEMENT

The authors declare that they have no relevant or material financial interests that relate to the research described in this paper

## AUTHORSHIP CONTRIBUTION STATEMENT

M. Malaki performed the experiments, T. Toraihi designed, supervised the project and wrote the manuscript, M. Ghorbani-Anarkooli helped in molecular biology, and A. Babaei helped in scaffold preparation.

## ACKNOWLEDGEMENT

This research was supported by Elite Researcher Grant Committee under award number [982787] from the National Institutes for Medical Research Development (NIMAD), Tehran, Iran,

we would like to express our deep gratitude and thanks to the NIMAD for their support. We appreciate the support of the Scientific Research and Technology Assistant of Tarbiat Modares University for this project, we thank them for their support.

The authors confirm that their research is supported by an institution that is primarily involved in education (Tarbiat Modares University) and research (NIMAD).

## FUNDING

This study was supported by a grant from Tarbiat Modares University for a PhD

decertation. This research was supported by Elite Researcher Grant Committee under award number [982787] from the National Institutes for Medical Research Development (NIMAD), Tehran, Iran

## DECLARATION

Authors have no conflict of interest to declare.

Table 1 demonstrates the sequences of forward and reverse primers of each gene with length of the fragment:

**Table 1** demonstrates the sequences of forward and reverse primers of each gene with length of the fragment:

Gene	Primers	Fragment size
<b>Primer pair Amy1 (exon 8,9)</b>	F: CAACCATGACAACCAGCGAGG R: TTGCCACAAGTGCTGTCTGAG	249 nucleotides
<b>Primer pair Cldn3</b>	F: CGTTTCGGCATTCATCGGCAG R: CTTGTACGCAGTTGGTACACTGG	236 nucleotides
<b>Primer pair cldn4</b>	F: TTTCTCAGTGCCCTCGCTCTC R: AAACCTGTCCAGCCACTCCAC	243 nucleotides
<b>Primer ki67 (exon11,12)</b>	F: ACGTGGGCTCCATTCTGTCTG R: ATTGGATTGCTGCTTTGCTGC	152 nucleotides
<b>Primer pair Cyclin D1 (exon3,4)</b>	F: CCAAAATGCCAGAGGCGGATG R: GAAAGTGCGTTGTGCGGTAGC	201 nucleotides
<b>Primer pair Dpt (exon1,2)</b>	F: CTGGTGGGAGGAGATCAACAGG R: TCGATCCAGCACTGACTCGAAG	109 nucleotides
<b>Primer pair Meox2 (exon1,2)</b>	F: GCGACAGTTCAGATTCCCAGG R: CCCGCTTCCACTTCATTCTCC	228 nucleotides
<b>Primer pair Aquaporin 5 (exone2,3)</b>	F: TGAACAACAACACAACGCCTGG R: AAGATCGGGCTGGGTTTCATGG	204 nucleotides
<b>Primer pair Pparg (exon4,5)</b>	F: AAGTGCCTTGCTGTGGGGATG R: AAATGCCTTGCCAGGGCTCG	149 nucleotides
<b>Primer pair Bpifa2e (exon3,4)</b>	F: CCATGCACAGAACAGCGTGAC R: AGCCAGCTTGAAGATCCAGG	131 nucleotides
<b>Primer pair -Tp63 (exon 4,5)</b>	F: CCATGCACAGAACAGCGTGAC R: TCTGGATGGGGCAGGTCTTTG	227 nucleotides

## REFERENCES

- [1] Napeñas JJ, Brennan MT, Fox PC. Diagnosis and treatment of xerostomia (dry mouth). *Odontology*, 2009; 97: 76-83.
- [2] Metzler MA, Venkatesh SG, Lakshmanan J, Carenbauer AL, Perez SM, Andres SA, Appana S, Brock GN, Wittliff JL, Darling DS. A systems biology approach identifies a regulatory network in parotid acinar cell terminal differentiation. *PloS one*, 2015; 10: e0125153.
- [3] Tanaka J, Senpuku H, Ogawa M, Yasuhara R, Ohnuma S, Takamatsu K, Watanabe T, Mabuchi Y, Nakamura S, Ishida S. Human induced pluripotent stem cell-derived salivary gland organoids model SARS-CoV-2 infection and replication. *Nature Cell Biology*, 2022; 24: 1595-1605.
- [4] Sugito T, Kagami H, Hata K, Nishiguchi H, Ueda M. Transplantation of cultured salivary gland cells into an atrophic salivary gland. *Cell transplantation*, 2004; 13: 691-700.

- [5] Kawakami M, Ishikawa H, Tachibana T, Tanaka A, Mataga I. Functional transplantation of salivary gland cells differentiated from mouse early ES cells in vitro. *Human cell*, 2013; 26: 80-90.
- [6] Chansaenroj A, Yodmuang S, Ferreira JN. Trends in salivary gland tissue engineering: from stem cells to secretome and organoid bioprinting. *Tissue Engineering Part B: Reviews*, 2021; 27: 155-165.
- [7] Tanaka J, Mishima K. In vitro three-dimensional culture systems of salivary glands. *Pathology International*, 2020; 70: 493-501.
- [8] Hieda Y, Iwai K, Morita T, Nakanishi Y. Mouse embryonic submandibular gland epithelium loses its tissue integrity during early branching morphogenesis. *Developmental dynamics*, 1996; 207: 395-403.
- [9] Hoffman MP, Kidder BL, Steinberg ZL, Lakhani S, Ho S, Kleinman HK, Larsen M. Gene expression profiles of mouse submandibular gland development: FGFR1 regulates branching morphogenesis in vitro through BMP-and FGF-dependent mechanisms. 2002.
- [10] Koyama N, Kashimata M, Sakashita H, Sakagami H, Gresik EW. EGF-stimulated signaling by means of PI3K, PLC $\gamma$ 1, and PKC isozymes regulates branching morphogenesis of the fetal mouse submandibular gland. *Developmental dynamics: an official publication of the American Association of Anatomists*, 2003; 227: 216-226.
- [11] Patel VN, Rebutini IT, Hoffman MP. Salivary gland branching morphogenesis. *Differentiation*, 2006; 74: 349-364.
- [12] Sakai T, Larsen M, Yamada KM. Fibronectin requirement in branching morphogenesis. *Nature*, 2003; 423: 876-881.
- [13] Ogawa M, Oshima M, Imamura A, Sekine Y, Ishida K, Yamashita K, Nakajima K, Hirayama M, Tachikawa T, Tsuji T. Functional salivary gland regeneration by transplantation of a bioengineered organ germ. *Nature communications*, 2013; 4: 2498.
- [14] Lombaert IM, Brunsting JF, Wierenga PK, Faber H, Stokman MA, Kok T, Visser WH, Kampinga HH, de Haan G, Coppes RP. Rescue of salivary gland function after stem cell transplantation in irradiated glands. *PloS one*, 2008; 3: e2063.
- [15] Lombaert IM, Knox SM, Hoffman MP. Salivary gland progenitor cell biology provides a rationale for therapeutic salivary gland regeneration. *Oral diseases*, 2011; 17: 445-449.
- [16] McCall AD, Nelson JW, Leigh NJ, Duffey ME, Lei P, Andreadis ST, Baker OJ. Growth factors polymerized within fibrin hydrogel promote amylase production in parotid cells. *Tissue Engineering Part A*, 2013; 19: 2215-2225.
- [17] Pradhan-Bhatt S, Harrington DA, Duncan RL, Jia X, Witt RL, Farach-Carson MC. Implantable three-dimensional salivary spheroid assemblies demonstrate fluid and protein secretory responses to neurotransmitters. *Tissue engineering Part A*, 2013; 19: 1610-1620.
- [18] Pradhan-Bhatt S, Harrington DA, Duncan RL, Farach-Carson MC, Jia X, Witt RL. A novel in vivo model for evaluating functional restoration of a tissue-engineered salivary gland. *The Laryngoscope*, 2014; 124: 456-461.
- [19] Chan Y-H, Huang T-W, Chou Y-S, Hsu S-H, Su W-F, Lou P-J, Young T-H. Formation of post-confluence structure in human parotid gland acinar cells on PLGA through regulation of E-cadherin. *Biomaterials*, 2012; 33: 464-472.
- [20] Chen MH, Chen YJ, Liao CC, Chan YH, Lin CY, Chen RS, Young TH. Formation of salivary acinar cell spheroids in vitro above a polyvinyl alcohol-coated surface. *Journal of Biomedical Materials Research Part A: An Official Journal of The Society for Biomaterials, The Japanese Society for Biomaterials, and The Australian Society for Biomaterials and the Korean Society for Biomaterials*, 2009; 90: 1066-1072.
- [21] Shin H-S, Kook Y-M, Hong HJ, Kim Y-M, Koh W-G, Lim J-Y. Functional spheroid organization of human salivary gland cells cultured on hydrogel-micropatterned nanofibrous microwells. *Acta biomaterialia*, 2016; 45: 121-132.
- [22] Adhikari N, Neupane S, Roh J, Aryal YP, Lee E-S, Jung J-K, Yamamoto H, Lee Y, Sohn W-J, Kim J-Y. Gene profiling involved in fate determination of salivary gland type in mouse embryogenesis. *Genes & genomics*, 2018; 40: 1081-1089.
- [23] Nakao A, Inaba T, Murakami-Sekimata A, Nogawa H. Morphogenesis and mucus

- production of epithelial tissues of three major salivary glands of embryonic mouse in 3D culture. *Zoological science*, 2017; 34: 475-483.
- [24] Li LT, Jiang G, Chen Q, Zheng JN. Ki67 is a promising molecular target in the diagnosis of cancer. *Molecular medicine reports*, 2015; 11: 1566-1572.
- [25] De Falco M, Fedele V, De Luca L, Penta R, Cottone G, Cavallotti I, Laforgia V, De Luca A. Evaluation of cyclin D1 expression and its subcellular distribution in mouse tissues. *Journal of Anatomy*, 2004; 205: 405-412.
- [26] Khalil W, Tiraihi T, Soleimani M, Baheiraei N, Zibara K. Conversion of neural stem cells into functional neuron-like cells by MicroRNA-218: Differential expression of functionality genes. *Neurotoxicity Research*, 2020; 38: 707-722.
- [27] Tiraihi T, Rezaie MJ. Apoptosis onset and bax protein distribution in spinal motoneurons of newborn rats following sciatic nerve axotomy. *International journal of neuroscience*, 2003; 113: 1163-1175.
- [28] Tiraihi T. Evaluation Of Protective Effects Of Alginate Hydrogel During Neurons Transdifferentiated From Bone Marrow Stromal Cells On Decrease Of Reactive Oxygene Specious. *Scientific Journal of Kurdistan University of Medical Sciences*, 2023; 28: 1-19.
- [29] Lopes S, Bueno L, AGUIAR FD, Finkler C. Preparation and characterization of alginate and gelatin microcapsules containing *Lactobacillus rhamnosus*. *Anais da academia brasileira de ciências*, 2017; 89: 1601-1613.
- [30] Matyash M, Despang F, Ikonomidou C, Gelinsky M. Swelling and mechanical properties of alginate hydrogels with respect to promotion of neural growth. *Tissue Engineering Part C: Methods*, 2014; 20: 401-411.
- [31] Rastogi P, Kandasubramanian B. Review of alginate-based hydrogel bioprinting for application in tissue engineering. *Biofabrication*, 2019; 11: 042001.
- [32] Kumar P, Nagarajan A, Uchil PD. Analysis of cell viability by the MTT assay. *Cold spring harbor protocols*, 2018; 2018: pdb. prot095505.
- [33] Diaz-Barrera A, Martinez F, Guevara Pezoa F, Acevedo F. Evaluation of gene expression and alginate production in response to oxygen transfer in continuous culture of *Azotobacter vinelandii*. *PLoS One*, 2014; 9: e105993.
- [34] Siburian M. The Encapsulation Effect on Viability of Mesenchymal Stem Cells. *Jurnal Farmasi Galenika (Galenika Journal of Pharmacy)(e-Journal)*, 2021; 7: 1-9.
- [35] Maioli E, Torricelli C, Fortino V, Carlucci F, Tommassini V, Pacini A. Critical appraisal of the MTT assay in the presence of rottlerin and uncouplers. *Biological Procedures Online*, 2009; 11: 227-240.
- [36] Rai Y, Pathak R, Kumari N, Sah DK, Pandey S, Kalra N, Soni R, Dwarakanath B, Bhatt AN. Mitochondrial biogenesis and metabolic hyperactivation limits the application of MTT assay in the estimation of radiation induced growth inhibition. *Scientific reports*, 2018; 8: 1531.
- [37] Riss TL, Moravec RA, Niles AL, Duellman S, Benink HA, Worzella TJ, Minor L. Cell viability assays. *Assay guidance manual [Internet]*, 2016.
- [38] Ghasemi M, Turnbull T, Sebastian S, Kempson I. The MTT assay: utility, limitations, pitfalls, and interpretation in bulk and single-cell analysis. *International journal of molecular sciences*, 2021; 22: 12827.
- [39] Toro M. Stability of alginate scaffolds for stromal and salivary gland epithelial cell growth. In: ed.^eds., 2022.
- [40] Hajiabbas M, D'Agostino C, Simińska-Stanny J, Tran SD, Shavandi A, Delporte C. Bioengineering in salivary gland regeneration. *Journal of biomedical science*, 2022; 29: 35.
- [41] Serrano Martinez P, Cinat D, van Luijk P, Baanstra M, de Haan G, Pringle S, Coppes RP. Mouse parotid salivary gland organoids for the in vitro study of stem cell radiation response. *Oral diseases*, 2021; 27: 52-63.
- [42] Hosseini ZF, Nelson DA, Moskwa N, Sfakis LM, Castracane J, Larsen M. FGF2-dependent mesenchyme and laminin-111 are niche factors in salivary gland organoids. *Journal of cell science*, 2018; 131: jcs208728.
- [43] Zhao C, Meng C, Cui N, Sha J, Sun L, Zhu D. Organoid models for salivary gland biology and regenerative medicine. *Stem Cells International*, 2021; 2021.
- [44] Jones SM, Kazlauskas A. Growth factor-dependent signaling and cell cycle progression. *Chemical Reviews*, 2001; 101: 2413-2424.



- [45] Villa A, Snyder EY, Vescovi A, Martínez-Serrano A. Establishment and properties of a growth factor-dependent, perpetual neural stem cell line from the human CNS. *Experimental neurology*, 2000; 161: 67-84.
- [46] Collins MK, Perkins GR, Rodriguez-Tarduchy G, Nieto MA, López-Rivas A. Growth factors as survival factors: regulation of apoptosis. *Bioessays*, 1994; 16: 133-138.
- [47] Edwards SN, Tolkovsky AM. Characterization of apoptosis in cultured rat sympathetic neurons after nerve growth factor withdrawal. *The Journal of cell biology*, 1994; 124: 537-546.
- [48] Pringle S, Van Os R, Coppes RP. Concise review: Adult salivary gland stem cells and a potential therapy for xerostomia. *Stem cells*, 2013; 31: 613-619.
- [49] Rotter N, Oder J, Schlenke P, Lindner U, Böhrnsen F, Kramer J, Rohwedel J, Huss R, Brandau S, Wollenberg B. Isolation and characterization of adult stem cells from human salivary glands. *Stem cells and development*, 2008; 17: 509-518.
- [50] Yi T, Lee S, Choi N, Shin H-S, Kim J, Lim J-Y. Single cell clones purified from human parotid glands display features of multipotent epitheliomesenchymal stem cells. *Scientific reports*, 2016; 6: 36303.
- [51] Savatier P, Malashicheva A. Cell-cycle control in embryonic stem cells. *Handbook of stem cells*, 2004; 1: 53-62.
- [52] Skrobanska R, Evangelatov A, Stefanova N, Topouzova-Hristova T, Momchilova A, Pankov R. Cell proliferation in in vivo-like three-dimensional cell culture is regulated by sequestration of ERK 1/2 to lipid rafts. *Cell proliferation*, 2014; 47: 336-346.
- [53] Matthew J, Vishwakarma V, Le TP, Agsunod RA, Chung S. Coordination of cell cycle and morphogenesis during organ formation. *Elife*, 2024; 13: e95830.
- [54] Crerar M, Swain WF, Pictet R, Nikovits W, Rutter W. Isolation and characterization of a rat amylase gene family. *Journal of Biological Chemistry*, 1983; 258: 1311-1317.
- [55] Delporte C, Bryla A, Perret J. Aquaporins in salivary glands: from basic research to clinical applications. *International journal of molecular sciences*, 2016; 17: 166.
- [56] Min S, Oyelakin A, Gluck C, Bard JE, Song E-AC, Smalley K, Che M, Flores E, Sinha S, Romano R-A. p63 and its target follistatin maintain salivary gland stem/progenitor cell function through TGF- $\beta$ /Activin signaling. *Iscience*, 2020; 23.
- [57] Kouwenhoven EN, van Bokhoven H, Zhou H. Gene regulatory mechanisms orchestrated by p63 in epithelial development and related disorders. *Biochimica Et Biophysica Acta (BBA)-Gene Regulatory Mechanisms*, 2015; 1849: 590-600.
- [58] Farahat M, Kazi GA, Taketa H, Hara ES, Oshima M, Kuboki T, Matsumoto T. Fibronectin-induced ductal formation in salivary gland self-organization model. *Developmental Dynamics*, 2019; 248: 813-825.